Dynamics of a Solidifying Icy Satellite Shell

J. J. Buffo[1], C. R. Meyer[1], and J. R. G. Parkinson[2]

[1]Thayer School of Engineering, Dartmouth College, Hanover, NH 03755, USA
[2]Atmospheric, Oceanic and Planetary Physics, Department of Physics, Clarendon Laboratory, University of Oxford, Parks Road, Oxford OX1 3PU, UK

Key Points:

- The ice-ocean interfaces of icy satellites likely exist as porous layers hydraulically connected to the underlying ocean.
- Interstitial brines likely exist in regions of planetary ice shells that are above their eutectic temperature.
- Thermochemical gradients in the porous basal layer of ice shells could provide a metabolic energy source for any potential organisms.

Corresponding author: Jacob Buffo, `jacob.j.buffo@dartmouth.edu`

Abstract

Ocean worlds have been identified as high-priority astrobiology targets due to the link between life and liquid water. Young surface terrain on many icy bodies indicates they support active geophysical cycles that may facilitate ocean-surface transport that could provide observables for upcoming missions. Accurately interpreting spacecraft observations requires constraining the relationship between ice shell characteristics and interior dynamics. On Earth, the composition, physical characteristics, and bioburden of ocean-derived ices are related to their formation history and parent fluid composition. In such systems the ice-ocean interface, which exists as a multiphase mushy layer, dictates the overlying ice's properties and evolution. Inclusion of the physics governing these boundaries is a novel strategy in modeling planetary ices, and thus far has been limited to 1D approaches. Here we present results from 2D simulations of an archetypal ice-ocean world. We track the evolution of temperature, salinity, porosity, and brine velocity within a thickening ice shell enabling us to place improved constraints on ice-ocean world properties, including: the composition of planetary ice shells, the thickness and hydraulic connectivity of ice-ocean interfaces, and heterogeneous dynamics/structures in the interfacial mushy layer. We show that stable eutectic horizons are likely a common feature of ice-ocean worlds and that ocean composition plays an important role in governing the structure and dynamics of the interface, including the formation of chemical gradient-rich regions within the mushy layer. We discuss the geophysical and astrobiological implications of our results and highlight how they can be validated by instrument specific measurements.

Plain Language Summary

Our solar system houses numerous ocean worlds that have the potential to harbor life. Typically these oceans reside beneath a thick global icy shell. Accordingly, much of what we know about these bodies relies on interpreting spacecraft observations of their icy exteriors. To illuminate the interior properties and dynamics of these worlds this requires an understanding of the relationship between internal processes and external observables. In ice-ocean environments the relationship between ice and ocean properties is governed by complex dynamics occurring at the ice-ocean interface. This interface is characterized by a slushy mixture of ice and brine (a mushy layer), who's physical structure, fluid flow, and chemical dynamics determine the resultant ice properties. Very few models of planetary ices include these dynamics, and so far there only exists one-dimensional models that do. Here we present the first two-dimensional model of planetary ices which includes the physics needed to accurately simulate the ice-ocean interface. We show that ice shell composition is governed by the two-dimensional dynamics of the ice-brine mushy layer, that the thickness of this layer scales directly with ice shell thickness, and that gradient rich regions in the mushy layer could provide sheltered and chemically favorable environments for organisms.

1 Introduction

The icy satellites of the outer solar system are some of the most enigmatic and inspirational bodies in planetary science, in large part due to their astrobiological potential (Des Marais et al., 2008; Hendrix et al., 2019; B. E. Schmidt, 2020). Ongoing geological activity and geomorphological features indicative of persistent subsurface water reservoirs suggests that these ice-ocean worlds may house aqueous environments suitable for the formation and evolution of life (Chivers et al., 2020; Hand et al., 2009; Marion et al., 2003; C. D. Parkinson et al., 2008; Porco et al., 2006; B. E. Schmidt, 2020; B. E. Schmidt et al., 2011). One of the most promising of these bodies is Europa (Hand et al., 2009, 2007; Marion et al., 2003; B. E. Schmidt, 2020). Europa likely possesses a global subsurface ocean ($\sim$100 km thick) underlain by a silicate mantle and roofed by a dynamic $\sim$10-30 km thick ice shell (Schubert et al., 2004). Serpentinization reactions at the benthic water-rock interface likely provide an ongoing source of reductants to the ocean, which, when coupled with surface generated oxidant delivery due to ice shell overturn (e.g. (Allu Peddinti & McNamara, 2015; Buffo et al., 2020; Johnson et al., 2017)), could facilitate redox disequilibrium chemistry favorable for metabolic processes (Vance et al., 2016). Furthermore, numerous geological features on Europa's surface suggest recent interaction with shallow subsurface water reservoirs (e.g. chaos (B. E. Schmidt et al., 2011; Sotin et al., 2002) and lenticulae (Chivers et al., 2020; Manga & Michaut, 2017; Michaut & Manga, 2014)) or even direct expression of ocean material (e.g. plumes (Jia et al., 2018; Sparks et al., 2016) and dilational bands (Howell & Pappalardo, 2018)), providing multiple opportunities to sample/observe underlying reservoir and/or ocean chemistry and any biosignatures that have been entrained in the upwelling cryohydrologic system (Kargel et al., 2000; B. E. Schmidt, 2020).

Europa is in good company in the outer solar system, as it is becoming increasingly apparent that oceans are a rather ubiquitous feature of icy satellites and dwarf planets beyond the frost line (Nimmo & Pappalardo, 2016; Buffo, 2019). Ganymede and Callisto likely house deep subsurface oceans, potentially sandwiched between layers of high pressure ices (Khurana et al., 1998; Vance & Brown, 2013). Enceladus' south pole likely possesses one of the shallowest (closest to the surface) oceans in the solar system (Nimmo, 2020), with its iconic tiger stripes ejecting potentially endogenic materials high enough above the moon's surface to be analyzed by the Cassini spacecraft's Cosmic Dust Analyzer, indicating the presence of a salty ocean in contact with the moon's silicate interior (Porco et al., 2006; Hansen et al., 2011; Waite et al., 2017). If geophysical processes facilitate transport between Titan's hydrocarbon laden surface and its putative subsurface ocean it could create an organic rich environment favorable for prebiotic chemistry (Fortes, 2000). Observations of active plumes and young terrain on Triton suggest it may possess a subsurface water reservoir (McKinnon & Kirk, 2014) (although these plumes may alternatively be generated by the solar heating of nitrogen ice (Kirk et al., 1990)), and the New Horizons flyby revealed geomorphological features on both Pluto and Charon that indicate the existence of either past or present interior oceans (Bierson et al., 2020; Hammond et al., 2016). Here, we utilize Europa as a well studied archetype for ice-ocean worlds, but note that our results are generally applicable and/or easily extendable to other ice-ocean systems.

A crucial component to understanding the geophysics, habitability, and biosignature expression mechanisms of Europa is constraining the physicochemical evolution of its ice shell (Allu Peddinti & McNamara, 2015; Hand et al., 2007; Kargel et al., 2000; B. E. Schmidt et al., n.d.; B. E. Schmidt, 2020; Vance et al., 2016). As the barrier to and facilitator of ocean-surface interaction, the material and transport properties of the ice shell will govern the geomorphological evolution of Europa's surface, the entrainment of ocean-derived impurities in the shell, and the chemistry of the underlying ocean (Buffo et al., 2020; Vance et al., 2016). Moreover, the ice shell will act as the primary observational medium for upcoming spacecraft missions (e.g. Europa Clipper, JUICE) (Pappalardo et al., 2017; Grasset et al., 2013), which makes quantifying the relationship between empirical ice shell properties and interior processes an imperative for optimal data interpretation and synthesis (e.g. (Kalousová et al., 2017)). However, while numerous investigations have emphasized the importance of physicochemical heterogeneities within and the material transport capabilities of the ice shell to both geophysical and potential astrobiological processes on Europa (e.g. (Barr & McKinnon, 2007; Han & Showman, 2005; Johnson et al., 2017; Kargel et al., 2000; Vance et al., 2020)) the structural and compositional details of the shell remain largely unconstrained. It is widely believed that Europa's ice shell is in a stagnant lid thermal regime; suggesting the presence of a thin (~3-5 km), brittle, ice lithosphere overlying a thicker (~10-30 km), ductile, isothermal icy mantle undergoing solid state convection (Barr & McKinnon, 2007; McKinnon, 1999; Schubert et al., 2004). Additionally, a number of investigations have highlighted likely trends in non-ice material distribution within Europa's ice shell (e.g. (Buffo et al., 2020; Kargel et al., 2000; Zolotov & Kargel, 2009)), with higher impurity entrainment in the shallow shell (Zolotov & Kargel, 2009) and around intrusive hydrological features within the shell (Buffo et al., 2020) and more efficient solute rejection as the ice shell thickened and ice-ocean interfacial growth rates slowed. Nevertheless, only

Buffo et al. (2020) provide quantitative estimates for the compositional profile of Europa's shell and themselves recognize the limitations of a one-dimensional model in an inherently multidimensional system (Buffo et al., 2021). A similar one-dimensional approach has been implemented to investigate the composition of Triton's ice shell by Hammond et al. (2018).

Multiphase reactive porous media, or 'mushy layers', play a fundamental and disproportionate role in the dynamics and evolution of both biogeochemical and geophysical systems (e.g. (Loose et al., 2011; Steefel et al., 2005; Tedesco & Vichi, 2014)). The ice-ocean layers of icy worlds, including Earth, are no exception. The complex reactive transport processes occurring near ice-ocean interfaces govern heat and mass transport between the two reservoirs and dictate the physicochemical properties of and impurity entrainment in the overlying ice (Buffo et al., 2020; Hunke et al., 2011; Thomas & Dieckmann, 2008). With direct implications for ice rheology (Assur, 1958; Durham et al., 2005), buoyancy (Han & Showman, 2005), eutectic point (McCarthy et al., 2011, 2007), bioburden (Santibáñez et al., 2019; Buffo, 2019; Brown et al., 2020), and conductivity (Kalousová et al., 2017) constraining the dynamics of ice-ocean/brine interfaces can improve our fundamental understanding of icy world geophysics and aid in spacecraft data analysis/interpretation (e.g. ice penetrating radar (Schroeder et al., 2016)). Furthermore, the ice-ocean interface of terrestrial ices provides a gradient rich substrate where both micro- and macro-fauna thrive in appreciable densities (Ackley & Sullivan, 1994; Daly et al., 2013; Spindler, 1994; Thomas & Dieckmann, 2003).

It has been suggested that the thick ice shells of low-gravity moons will support thicker multiphase boundary layers at their ice-ocean interfaces (on the order of meters to tens of meters), as this layer's thickness is inversely proportional to the interfacial thermal gradient (Buffo et al., 2021). This is supported by observations of columnar sea ice formed beneath the Ross Ice Shelf, which exhibited brine channels, high impurity entrainment, and hydraulic connectivity to the underlying ocean throughout the bottom 6 m of ice (Zotikov et al., 1980). Convective overturn of high salinity brine in these porous boundary layers leads to the formation of heterogenous channel structures within the ice matrix (Cottier et al., 1999; Wells et al., 2011; Wettlaufer et al., 1997) and can produce brinicles that extend into the underlying ocean from the basal ice surface (Cartwright et al., 2013). As cold, saline brine is convected out of the mushy layer in localized downwelling plumes it acts as a heat sink for the surrounding seawater, in some cases depressing the local temperature enough that an ice membrane forms around the saline fluid (e.g. (Mahadevan, 2017)). These tubular ice membranes produce regions with exceptionally high thermal and chemical gradients that could serve as an oasis for biology, akin to terrestrial hydrothermal and chemical garden systems (Cartwright et al., 2013; Vance et al., 2019). This possibility is strengthened by the fact that the ice-ocean interface will be the site of oxidant delivery to the ocean, providing a redox boon for any potential organisms (Allu Peddinti & McNamara, 2015; Vance et al., 2016).

Understanding the structure and dynamics of the ice-ocean interface of icy worlds has both geophysical and astrobiological implications (Buffo et al., 2021, 2020). It is a mandatory port of call for ocean-surface interaction, a core-mantle boundary in the cryospheric system that could facilitate regional geomorphological heterogeneities, and likely one of the most habitable environments on high priority astrobiology targets. Here, we simulate the multiphase two-dimensional evolution of Europa's ice-ocean interface. We provide improved constraints on the compositional profile of the growing ice shell and the relationship between ice-ocean interface thermal gradient and impurity entrainment. We show that the multiphase ice-ocean boundary layer thickens as Europa's ice shell thickens and interfacial thermal gradients decrease. Additionally, we show that brinicles are a likely byproduct of the convective overturn of brine in the porous basal ice layer. Finally, we discuss how our estimations of ice shell structure and composition can be utilized to improve geophysical models, constrain the habitability, and aid in spacecraft mission planning and data analysis of Europa and other icy worlds.

2 Methods

To simulate the two-dimensional evolution of Europa's ice-ocean interface we use the reactive porous media model SOFTBALL: SOlidification, Flow, and Thermodynamics in Binary ALLoys. First introduced in J. R. G. Parkinson, Martin, Wells, and Katz (2020), SOFTBALL is an open source code capable of efficiently simulating the phase evolution, heat transport, and mass transport in mushy layers. The code has been tested extensively (cf. (J. R. G. Parkinson, 2019; J. R. G. Parkinson, Martin, Wells, & Katz, 2020; Wells et al., 2019)), and we provide an additional validation of the model's ability to reproduce the compositional and structural properties of terrestrial sea ice in Supplementary Section S1.

The equations governing the evolution of ice-ocean interfaces are well documented in the literature (e.g. (Feltham et al., 2006; Hunke et al., 2011; Worster, 1997). Employing the Boussinesq approximation and assuming no phase change driven flow (ρ_{br}=ρ_i, where ρ_{br} is brine density, and ρ_i is ice density), conservation of mass in a reactive porous media requires

$$\boldsymbol{\nabla} \cdot \boldsymbol{q} = 0 \tag{1}$$

where $\boldsymbol{q} = (u, v)$ is the two-dimensional Darcy velocity. We assume the ice matrix is rigid and immobile and restrict mass transport to the fluid phase. Fluid flow is governed by the incompressible form of Darcy's law

$$\boldsymbol{q} = -\frac{\Pi}{\mu}\left(\nabla p + \rho_{br}\boldsymbol{g}\right) \tag{2}$$

where Π is permeability (typically a function of porosity, here we utilize the Kozeny-Carman relationship given in J. R. G. Parkinson, Martin, Wells, and Katz (2020), see Eq. 7 below), μ is the dynamic viscosity of the brine, p is dynamic pressure, and $\boldsymbol{g}$ is gravity. Conservation of energy is given by

$$\overline{\rho c}\frac{\partial T}{\partial t} = -\rho_{br}c_{br}\boldsymbol{q}\cdot\nabla T + \nabla\cdot\left(\bar{k}\nabla T\right) - \rho_i L\frac{\partial \phi}{\partial t} \tag{3}$$

where c is specific heat, T is temperature, k is thermal conductivity, and L is the latent heat of the water-ice phase transition. Quantities with overbars are volume averaged quantities (i.e. $\bar{k} = \phi k_{br} + (1-\phi)\,k_i$, where ϕ is liquid fraction (porosity)). This equation accounts for heat transport via advection and diffusion as well as the generation/usage of heat due to freezing/melting. Similarly, the conservation of salt is given by

$$\phi\frac{\partial C}{\partial t} = -\boldsymbol{q}\cdot\nabla C + \nabla\cdot(D\nabla C) - C\frac{\partial \phi}{\partial t} \tag{4}$$

where C is brine concentration, and D is the diffusion coefficient of the solute. We assume no salt is present in the ice phase, in line with contemporary approaches (Feltham et al., 2006; J. R. G. Parkinson, Martin, Wells, & Katz, 2020). This allows for evolution of the brine phase via advection, molecular diffusion, and concentration/dilution caused by freezing/melting of ice. The system of Equations 1-4 can be closed by assuming that the system obeys an idealised eutectic phase diagram (Figure 1a), which relates brine concentration to temperature and liquid fraction. We follow the methodology of (J. R. G. Parkinson, Martin, Wells, & Katz, 2020) (their Section 2.2 and Appendix A), and define the liquidus and solidus curves by

$$T_L(C) = T_m - mC \tag{5}$$

$$T_{Sol}(C) = T_m - mC_e \tag{6}$$

where T_L is the liquidus temperature, T_m is the freezing temperature of pure water, m is a solutal freezing point depression coefficient with units of K kg g^{-1} (equivalently, K ppt^{-1}), T_{Sol} is the solidus temperature, and C_e is the eutectic composition. If the temperature is above the liquidus the system will be a fluid ($\phi = 1$), if it is below the solidus the system will be a solid ($\phi = 0$) and any residual salt is assumed to exist as a hydrated solid phase. Between these curves the system will exist as a mixture of pure ice and brine with a concentration governed by Equation 5.

Here we simulate the top-down solidification of a hypothetical Europan ocean using the initial and boundary conditions presented in Figure 1b and the physical parameter values given in Table 1. We have chosen to use an ocean with a salinity of 35 ppt and linear liquidus slope of -0.048 K/ppt as this lies comfortably within the range of predicted Europan ocean concentrations (Hand & Chyba, 2007; Zolotov & Shock, 2001) and compositions (Trumbo et al., 2019; Zolotov & Shock, 2001). Simulations are initiated as a completely fluid filled domain subject to an undercooled upper boundary (T_s=100 K) which induces the formation of an ice shell. Throughout the simulation SOFTBALL tracks the evolving temperature (T), bulk salinity (C), porosity (ϕ), and velocity (u, v) within the system. By assuming the domain exists as a thin Hele-Shaw cell a finite fluid permeability (J. R. G. Parkinson, Martin, Wells, & Katz, 2020)

$$\Pi(\phi) = \left\{ \frac{12}{d^2} + \left[\frac{K_0 \phi^3}{(1-\phi)^2} \right]^{-1} \right\}^{-1} \tag{7}$$

allows us to solve for flow throughout the entire domain using Darcy's law (Eq. 2). K_0 is a permeability factor and d is the Hele-Shaw cell spacing. While an important factor in governing the dynamic evolution of ice-brine mushy layers (Buffo et al., 2021, 2020), as it dictates the advection of heat and solutes throughout the system, the precise permeability-porosity relationship of ocean-derived ices remains under constrained and an active topic of research in both terrestrial and planetary ice science (Golden et al., 2007; McCarthy et al., 2013, 2007). Our selected permeability-porosity relationship is consistent with previous studies of ice-ocean mushy layer systems (e.g. (Katz & Worster, 2008; J. R. G. Parkinson, Martin, Wells, & Katz, 2020)) and agrees well with power law permeability-porosity relationships ($\Pi(\phi) \propto \phi^n$, where $n \in [1, 3]$) that have been adopted by other studies of ice shell mushy layers (e.g. (Buffo et al., 2020; Hammond et al., 2018)) for porosities representative of mushy layer interiors ($\phi < 0.8$, see Figure 4 of Katz and Worster (2008) and Supplementary Figure S4). The value of the permeability factor implemented here, $K_0 = 2 \times 10^{-9}$ m^2, was selected such that it reproduces bulk salinity values and trends observed in terrestrial sea ice (see Supplementary Section S1 and Supplementary Figure S3). Moreover, this value is in agreement with reference permeabilities used in previous studies (e.g. $K_{ref} = 10^{-9}$ m^2 in Hammond et al. (2018) and Golden et al. (2007)). Nevertheless, both permeability-porosity relationships and potential percolation thresholds - the limitation of fluid flow below a critical porosity (Golden et al., 2007) - have substantial implications for the dynamics and evolution of mushy layers (Buffo et al., 2021, 2020) and constraining their values will be essential for improving the accuracy of planetary ice shell models.

The Hele-Shaw cell approach optimizes computation speed as the Darcy equation is simpler to solve than the full Navier-Stokes (a noted challenge for mushy layer systems (Chung & Worster, 2002)) and restricting flow in the underlying fluid permits the use of larger CFL-limited time steps. Additionally, it limits phase boundary effects (removing the need to define interfacial conditions between the fluid and porous regions, e.g. multiple domain Stokes-Darcy approaches (Le Bars & Worster, 2006)) while ensuring the underlying fluid has an amplified permeability such that downwelling plumes will not stagnate and artificially impact the evolution of the overlying porous region (Supplementary Section S4). Previous works have implemented this approach to simulating mushy layers (e.g. (Wells et al., 2019; Katz & Worster, 2008)). It should be noted that the numerical solutions in the underlying fluid are inherently less realistic than those in the mushy layer due to the implementation of a finite permeability. As such, results of structural and dynamic evolution in the free fluid region should be interpreted with this in mind. We discuss the limitations of the Hele-Shaw cell approach in describing the dynamics of the underlying fluid at length in Supplementary Section S4.

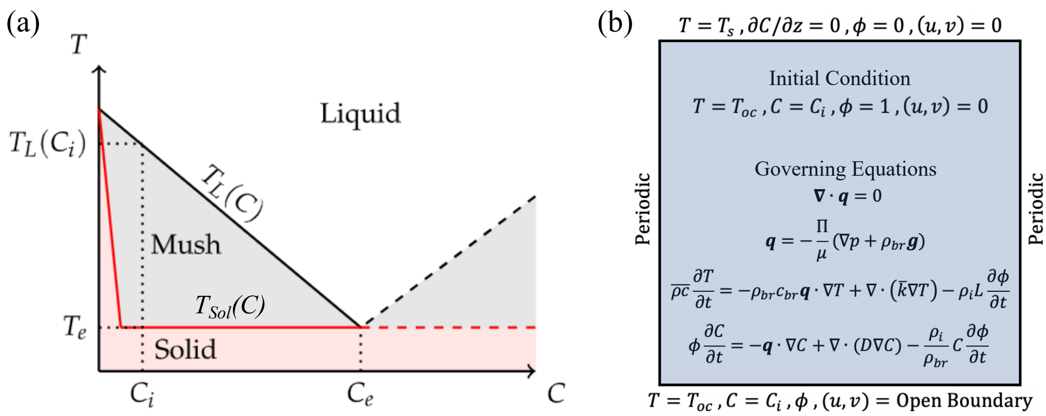

Figure 1. **(a)** – Idealized eutectic phase diagram for the ice-brine system. Above the liquidus, $T_L(C)$, the system exists as a pure fluid. Below the solidus, $T_{Sol}(C)$, the system is composed of solid ice and solid salts. Between these regions the system exists as a two-phase mush of solid ice and concentrated brine. **(b)** – Initial and boundary conditions utilized in the top-down solidification simulations.

3 Results

3.1 Bulk Salinity of Europa's Ice Shell and its Relation to Thermal Gradient

To constrain the bulk salinity of Europa's ice shell we simulated the top-down solidification of the shallow shell (0-1.1 km) using twelve different domain sizes (ranging from 10 m x 10 m to 2 km x 250 m) and resolutions (ranging from 3.9 cm to 7.8 m). The consistency of results across a range of resolutions further validates the model's ability to accurately capture the continuum mechanics that govern the system, even in simulations where small scale heterogeneities such as brine channels are not explicitly resolved. An example of the two-dimensional bulk salinity and porosity profiles produced by such a run can be seen in Figure 2. This particular simulation was conducted using a 20 m by 20 m domain at a resolution of 3.9 cm (resolution results from a 512 x 512 grid) and covers the uppermost portion of the ice shell (0-20 m). Both fossilized and active high salinity regions can be seen throughout the thickness of the forming ice shell, suggesting a heterogeneous and appreciable distribution of salt within the ice. It is important to note that there may be additional substructure within these regions not captured at the current simulation resolution (brine channels in natural sea ice on Earth are typically ∼1-3 mm in diameter), however the den-

Variable	**Definition**	**Value**
$\boldsymbol{\beta}$	Density coefficient for salt	5.836e-4 kg ppt^{-1}
$\boldsymbol{c}$	Specific heat of the ocean	3985 J kg^{-1} K^{-1}
$\boldsymbol{c_{br}}$	Specific heat of ice	2000 J kg^{-1} K^{-1}
$\boldsymbol{C_e}$	Eutectic composition	230 ppt
$\boldsymbol{C_i}$	Ocean composition	35 ppt
$\boldsymbol{d}$	Hele-Shaw cell spacing	5e-5 m
$\boldsymbol{\eta}$	Dynamic viscosity	1.88e-3 Pa s
$\boldsymbol{g}$	Gravity	1.32 m s^{-2}
$\boldsymbol{H}$	Scale height	(varies) m
$\boldsymbol{k_{br}}$	Thermal conductivity of the ocean	0.6 W m^{-1} K^{-1}
$\boldsymbol{k_i}$	Thermal conductivity of ice	2.0 W m^{-1} K^{-1}
$\boldsymbol{k_s}$	Salt diffusivity in water	2e-9 m^2 s^{-1}
$\boldsymbol{K_0}$	Permeability factor	2e-9 m^2
$\boldsymbol{L}$	Latent heat of fusion	334774 J kg^{-1}
$\boldsymbol{m}$	Linear liquidus slope	0.048 K ppt^{-1}
$\boldsymbol{\phi_s}$	Surface porosity	0
$\boldsymbol{\phi_{oc}}$	Ocean porosity	1
$\boldsymbol{p_s}$	Partition coefficient	0.001
$\boldsymbol{\rho_{br}}$	Brine density	1000+1000$\times\boldsymbol{\beta}\times\boldsymbol{C}$ kg m^{-3}
$\boldsymbol{\rho_i}$	Ice density	917 kg m^{-3}
$\boldsymbol{T_e}$	Eutectic temperature	273.15 - $\boldsymbol{m}\times\boldsymbol{C_e}$ K
$\boldsymbol{T_{oc}}$	Ocean temperature	273.15 - $\boldsymbol{m}\times\boldsymbol{C_i}$ + 0.01 K
$\boldsymbol{T_s}$	Surface temperature	100 K

Table 1. Variables used by the SOFTBALL code. The scale height, H, is used to define the simulation domain size and nondimensionalize the system.

dritic structure and density distribution (channel collapse as the ice thickens) of the high salinity regions matches both observations and theoretical predictions of ice-ocean systems (Rees Jones & Worster, 2013; Wells et al., 2011, 2019; Worster & Rees Jones, 2015; Middleton et al., 2015). Also apparent is the existence of a thin (in relation to the overall ice thickness), dynamic mushy layer at the ice-ocean interface. The convective overturn of brine within this layer (Figure 2b) is responsible for the desalination of, and thus the level of ocean-derived material entrainment in, the ice shell (Buffo et al., 2020; Wells et al., 2019; Wettlaufer et al., 1997; Worster, 1997). Darcy velocities within the mushy layer range from $\sim 10^{-11}$ m/s near the ice-mush interface where porosity approaches zero and $\sim 10^{-6}$ m/s in the downwelling saline plumes.

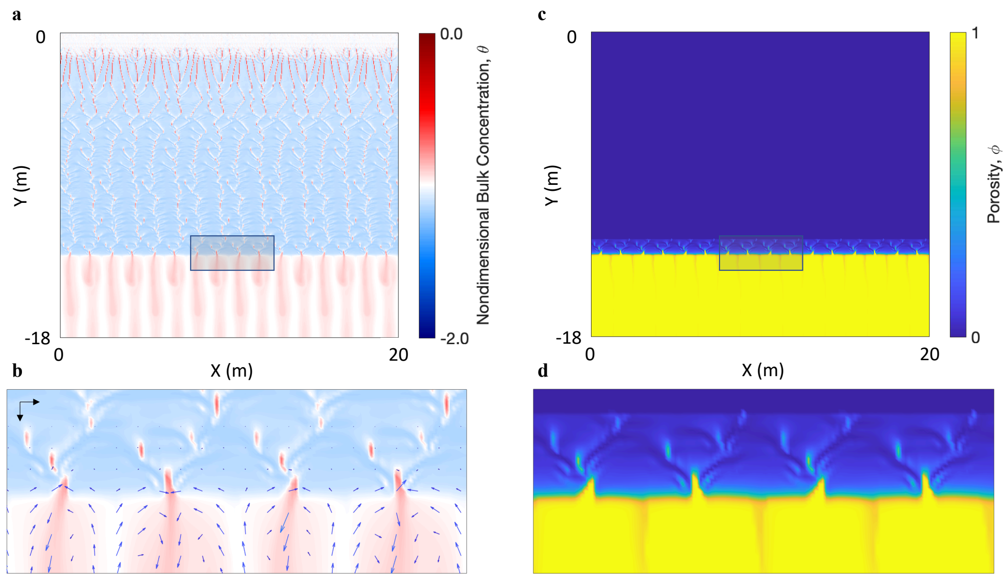

Figure 2. The compositional (bulk salinity) and structural (porosity) profile in Europa's growing ice shell. **a)** Two-dimensional nondimensionalized bulk salinity profile using a scale height, H, of 10 m (domain size: 18m x 20m). Where nondimensional bulk salinity, $\theta = \frac{C - C_e}{C_e - C_i}$. Fossilized high salinity regions can be seen in the upper ice and dense, high salinity plumes can be seen emanating from the ice-ocean interface. **b)** Magnified view of the shaded box in panel (a), with velocity vectors included, showing the convective overturn of brine within the interfacial mushy layer. For scale, black arrows in the top left have lengths that represent Darcy velocities of 10^{-6} m/s **c)** Two-dimensional porosity profile for the same region depicted in panel (a). **d)** Magnified view of the shaded box in panel (c). Low porosity brine channels are associated with high salinity downwellings.

To investigate how the ice shell composition varies with depth we horizontally average the bulk salinity of each two-dimensional run and plot it against it's corresponding location within the shell (Figure 3a-c). It can be shown that the temperature profile in the forming ice varies negligibly from a simple conductive (linear) profile (See Supplementary Section S2), and thus the ice-ocean interface thermal gradient is well represented by

$$\frac{\partial T}{\partial z} = \frac{T_{oc} - T_s}{H_{shell}}, \tag{8}$$

where T_{oc} is ocean temperature, T_s is surface temperature, and H_{shell} is the depth of the ice-ocean interface from the surface. Plots of bulk salinity as a function of interfacial thermal gradient can be found in Figure 3d-f. The functional form of the best fit lines closely follow the analytical solutions derived by Buffo et al. (2020) (Equations 26 & 27 of their manuscript) for the compositional evolution of a simplified ice-ocean system. Here we implement a Levenberg-Marquardt algorithm to relate bulk salinity and depth within the ice shell using the equation

$$C(z) = a + \frac{b}{c - z}[1 - d\exp(-fz)] \tag{9}$$

where C is bulk salinity, z is depth within the shell, and a, b, c, d, and f are constant coefficients that account for stretches and translations. Similarly, we relate bulk salinity to thermal gradient using the equation

$$C\left(\frac{\partial T}{\partial z}\right) = a + \frac{b\left(\frac{\partial T}{\partial z} + c\right)}{\left(d + f\frac{\partial T}{\partial z}\right)}\left[1 - h\exp\left(\frac{-j}{\frac{\partial T}{\partial z}}\right)\right], \tag{10}$$

where a, b, c, d, f, h, and j are constant coefficients that account for stretches and translations.

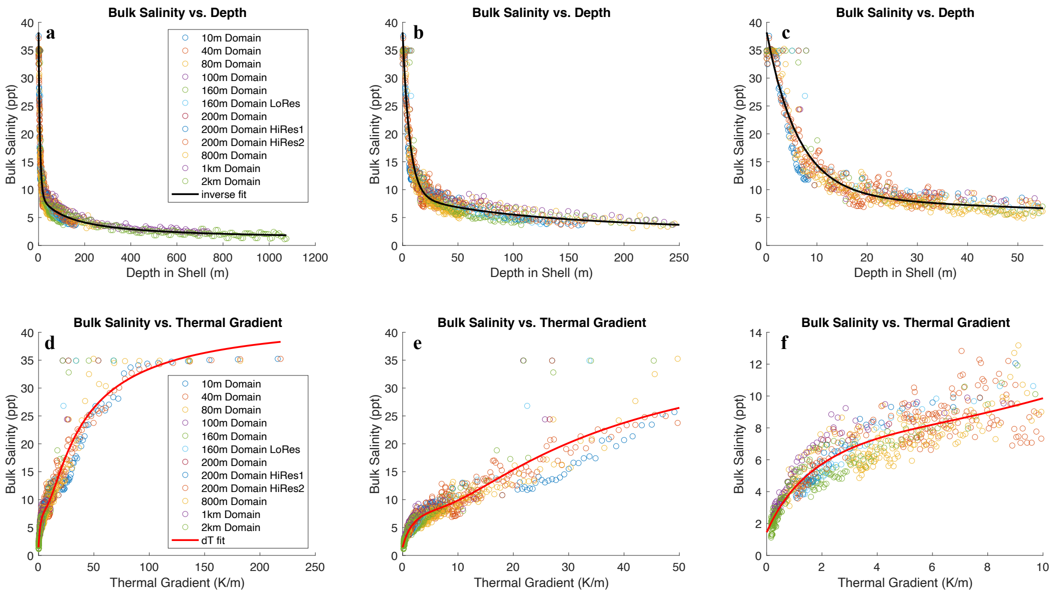

Figure 3. Bulk salinity characteristics of Europa's ice shell for a 35 ppt ocean. **a-c)** Bulk salinity variation with depth in the shell. High salinity values near the surface quickly decrease with depth and asymptotically approach a lower limit of 0.984 ppt, according to the best fit line of Equation 9 (coefficients: a=0.984, b=-1014, c=-123.4, d=-3.529, f=0.1529). **d-f)** Bulk salinity variation with ice-ocean interface thermal gradient (assuming a conductive profile in the overlying ice shell). At large thermal gradients (>100 K/m) all salt is trapped within the ice. There is a prominent 'shoulder' region between 3-10 K/m that is captured well by the fit line of Equation 10 (coefficients: a=7.864, b=-2576, c=-5.148, d=-2067, f=-869.2, h=-10.9, j=27.2). This regime could be indicative of a transition between dominant desalination mechanisms in the mushy layer (Buffo et al., 2020, 2021). (Note: Two data points with bulk salinity >35 ppt visible in panels (a-c) do not appear in panels (d-f) as they are the result of interfacial thermal gradients which exceed 250 K/m. These results negligibly affect the fit lines of Equations 9 and 10 while highlighting the difficulty of accurately simulating extreme thermal environments, as we expect these values to be 35 ppt)

The simulated bulk salinity values are well approximated by the functional forms of Equation 9 & 10, and exhibit a number of important trends and features predicted by earlier studies (e.g. (Buffo et al., 2020)). These include a trend toward compositional homogeneity as the ice shell thickens and interfacial thermal gradients decrease; a nonzero lower limit for entrainment rate (0.98 ppt as $z \to \infty$ and 1.45 ppt as $\partial T/\partial z \to 0$), as predicted by Equations 9 & 10, respectively); one hundred percent salt retention when ice forms under large thermal gradients (representative of rapid freezing); and the existence of transitional regimes in mushy layer dynamics (evidenced by the 'shoulder' region of Figure 3e). These properties and their implications for the geophysics and astrobiology of Europa and other ice-ocean worlds are discussed in Section 4.

3.2 Ice-Ocean Interface Mushy Layer Thickness

The porous region near the ice-ocean interface (e.g. Figure 2d) plays an important role in governing the properties and evolution of the ice shell. This dynamic region dictates the chemical composition and physical structure of forming ice, governs heat and solute transport between the ocean and ice shell reservoirs, and determines the hydraulic connectivity of the deep ice shell. Studies suggest that the properties of this layer are dynamic and evolve as the overlying ice cover thickens and interfacial thermal gradients decrease (e.g. (Buffo et al., 2021)). Furthermore, the environmental parameters (e.g. gravity, ocean composition) of a given system will impact the layer's structure, suggesting that a diverse array of deep ice shell environments exist across the solar system and throughout individual ice-ocean world's lifetimes.

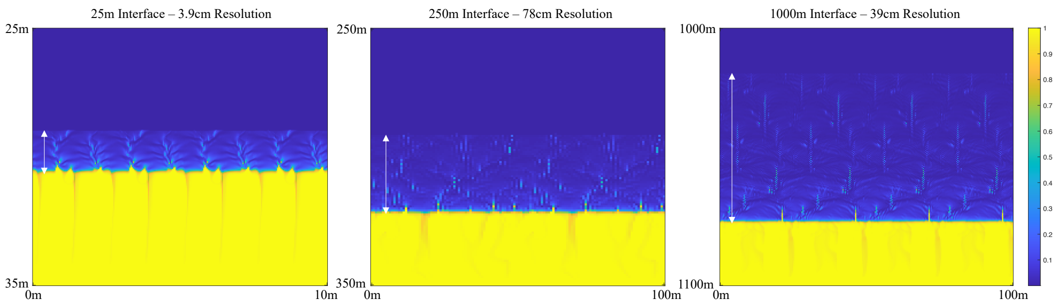

Figure 4. Thickness and structure of the ice-ocean interface mushy layer at various depths within the ice shell. The mushy layer thickness increases as the ice shell thickens, consistent with previous observations and theory (Buffo et al., 2021; Wells et al., 2011). The majority of fluid motion is concentrated in a high porosity region near the base of the mushy layer (e.g. Figure 2b), resulting in a 'stagnant' region with decreased fluid flow underlain by a thin convecting boundary layer. This was predicted theoretically by Worster (1991) for systems with large mush Rayleigh numbers, which is the case for the mushy layers considered here (see Supplementary Section S3). White arrows demarcate the horizontally averaged mushy layer thickness. (Note: The left image depicts a 10 m x 10 m domain while the center and right images depict a 100 m x 100 m domain.)

To constrain the evolving thickness of Europa's ice-ocean interface mushy layer we slightly modified the boundary conditions presented in Figure 1 such that the upper thermal boundary was governed by a Neumann (gradient/flux) boundary condition ($\partial T/\partial z = (T_{oc} - T_s)/H_{shell}$) and carried out high resolution, top-down solidification simulations for descending depths within the shell (H_{shell} = 0 m, 25 m, 50 m, 100 m, 250 m, 500 m, and 1000 m). Porosity profiles during three of these runs can be seen in Figure 4. Periodically

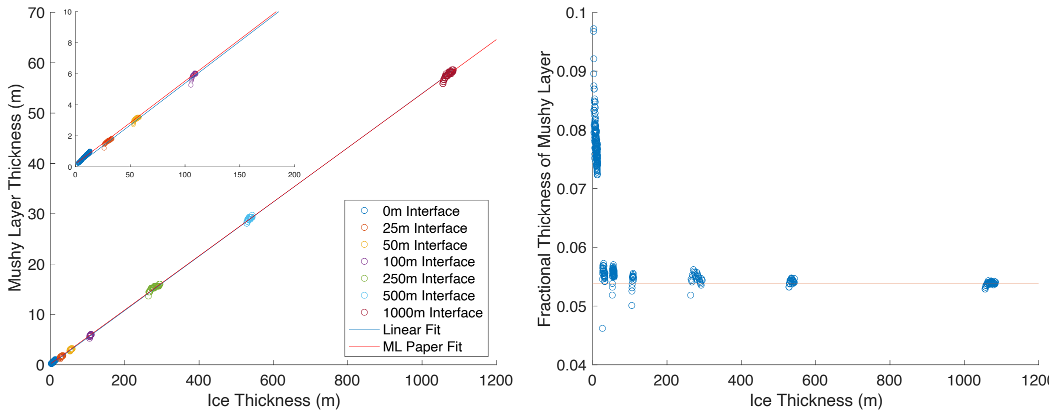

Figure 5. Ice-ocean interface mushy layer thickness and its relationship to ice shell thickness. **(Left)** Mushy layer thicknesses recorded during seven simulations, each initiated with a different ice-ocean interface position (overlying ice shell thickness, H_{shell}). The relationship between mushy layer thickness and ice shell thickness is well captured by the fit line of Equation 11, here 'ML Paper Fit'. A simple linear relationship also closely matches the data, evidenced by its overlap with the fit line of Equation 11 until the plot is magnified. ('ML Paper Fit' coefficients: a=0.02685, b=-11.64, c=-62.28; linear relationship=0.0539). Inset – magnified view of the shallow ice shell region (0-200 m). **(Right)** The fractional percentage of the ice shell occupied by the mushy layer. The red line corresponds to the linear fit trend of 0.0539.

during these runs the porosity profile was horizontally averaged and the region satisfied by $1e{-5} < \phi < 0.95$ was measured, giving the mushy layer thickness. These bounds were selected in lieu of $0 < \phi < 1$ to avoid measuring any residual low porosity regions in the upper ice shell and any high porosity structures extending from the ice-ocean interface (e.g. brinicles - the focus of Section 3.3). The relationship between ice-ocean interface mushy layer thickness and ice shell thickness can be seen in Figure 5a. Figure 5b shows the fraction of the ice shell occupied by the mushy layer and its relationship to ice shell thickness. The increase in mushy layer thickness with growing ice shell thickness is well fit by the analytical solution derived by (Buffo et al., 2021), (modified from Equation 25 of (Buffo et al., 2021)):

$$h_{ML} = aH_{shell}\left(1 + \sqrt{1 - \frac{b}{H_{shell}} - \frac{c}{H_{shell}^2}}\right) \tag{11}$$

where h_{ML} is mushy layer thickness, H_{shell} is ice shell thickness, and a, b, and c are constants that allow for translations and stretches. The relationship between mushy layer thickness and ice shell thickness is also well approximated by a simple linear trend (relationship coefficient $= 0.0539$). This suggests that accretionary regions of Europa's ice shell likely possess a substantial multiphase ice-ocean boundary layer that occupies as much as 5% of the ice shell thickness. Notably, the linear relationship coefficient closely matches the eutectic horizon predicted by assuming a conductive (linear) thermal profile within the ice shell ($h_{eut} = \frac{T_{oc}-T_e}{T_{oc}-T_s} = 0.0548$). While slightly overestimating the mushy layer's thickness, eutectic horizons likely provide an exceptional first order estimate of ice shell hydrological structure. This has important implications for regional and global geophysical processes, ocean-derived material entrainment in the shell, and Europa's potential habitability (further discussed in Section 4).

3.3 Fine Scale Heterogeneities and Brinicle Formation

The fine scale structure in the multiphase region near the ice-ocean interface (e.g. Figure 2) supports thermochemical gradients that when combined with the porous nature of the ice-brine matrix could provide an ample substrate for any potential organisms. Vance et al. (2019) suggested that brinicles (hollow tubes of ice formed around downwelling brine plumes) could form at the ice-ocean interfaces of icy worlds and result in chemical garden like structures. Similar to the hydrothermally formed chemical garden systems at Earth's seafloor, an oasis for life (Barge et al., 2015; Cartwright et al., 2002), brinicles and the mushy layer they grow from could provide a gradient rich habitat for an inverted benthic community (Cartwright et al., 2013).

To investigate the physicochemical properties of brinicles on Europa we performed high resolution simulations of the ice-ocean interface for a number of overlying ice shell thicknesses (similar to Section 3.2). The resulting porosity, brine salinity, and salinity gradient profiles for three such simulations are depicted in Figure 6. Brinicle structures can be seen extending from the mushy layer in all three cases (left column of Figure 6). The size of the brinicle structures increases with ice shell thickness. This is consistent with the convective patterns in a thickening mushy layer, where downwellings drain an increasingly large region of the mushy layer as brine channel spacing increases. Brinicle size may also be affected by their longevity. The ice-ocean interface is quite dynamic and brinicle structures grow and disappear repeatedly during simulations. The timescale over which this cycling occurs increases with depth, suggesting a thicker ice shell may promote the formation of larger and more stable 'brinicle gardens'. The lifetimes of brinicles at an ice-ocean interface depth of 10 m, 50 m, and 1000 m are on the order of hours, days, and years, respectively. Salinity gradients are highest near brine channels within the mushy layer and at the edges of downwelling high salinity plumes, the distribution and geometry of which mirror those imaged in laboratory experiments of directional solidification of brine in a Hele-Shaw cell (Middleton et al., 2015). While the brinicle structures themselves do not house large salinity gradients, they form directly adjacent to regions that do (downwelling plumes). This is expected as brinicle formation is a result of the difference between thermal and molecular diffusivity in the system (Cartwright et al., 2013).

It is important to note, however, that brinicles on Earth only occur near land, in sheltered water where currents are low. Stronger currents induce turbulent mixing near the ice-ocean interface, dissipating the downwelling plumes and preventing brinicle formation. Given the substantial latitudinal currents predicted for icy satellites in the outer solar system (e.g. (Soderlund et al., 2014; Soderlund, 2019)) it is quite possible that brinicles may not be able to form. Conversely, the gradient rich brine channels within the mushy layer are protected from the underlying shear flow by the surrounding ice matrix. This suggests a putative ice-ocean interface habitat more akin to the terrestrial infaunal benthos rather than the extensional structures of chemical gardens. The importance of the ice-ocean interface as a potentially habitable environment on icy worlds as well as potential limitations of the current model in simulating brinicle geometry and evolution is discussed in Section 4 and Supplementary Section S4, respectively. Briefly, the implementation of Darcy's law throughout the domain (Equation 2) will under predict fluid velocities in the underlying ocean, potentially impacting downwelling plume dynamics and altering the formation and evolution of brinicles, as these structures exist in and interact with the free fluid beneath the ice-ocean interface mushy layer.

4 Discussion

The ability to simulate, at high resolution, the two-dimensional evolution of Europa's ice-ocean interface offers insight into the important role this boundary plays on icy worlds. A few examples are: the distribution of ocean-derived material within the ice shell; the relationship between impurity entrainment and ice-ocean interfacial thermal gradient; the

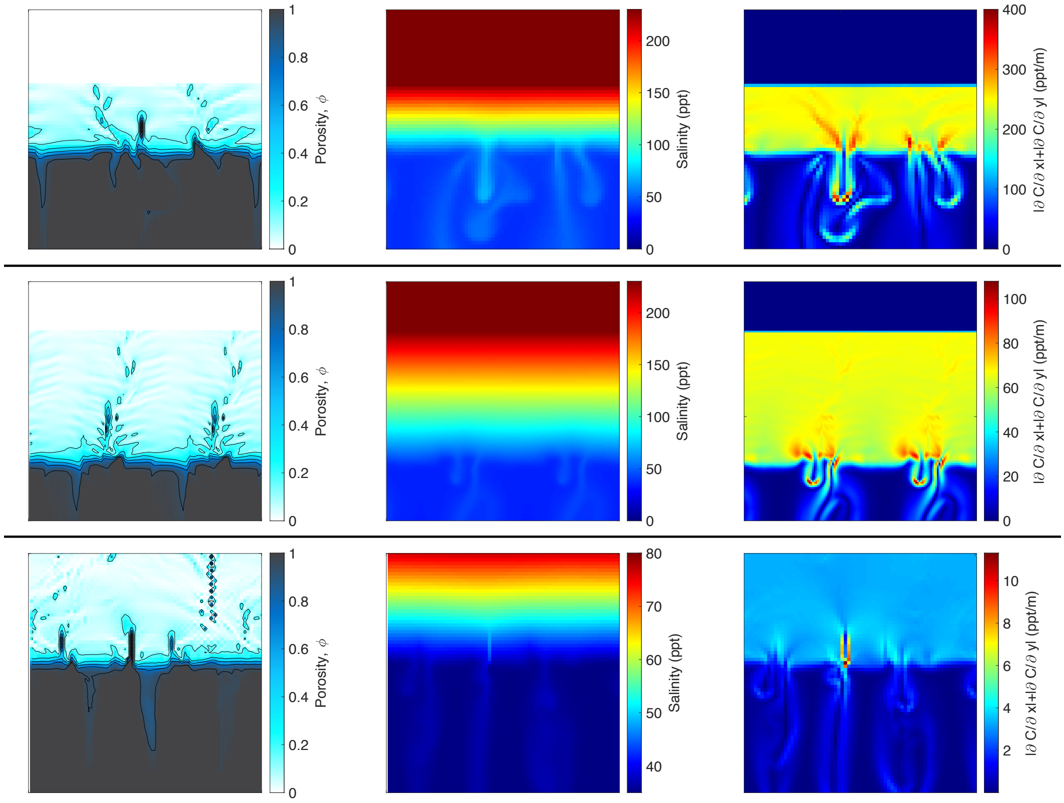

Figure 6. The physicochemical properties of brinicles on Europa. **(Top-Bottom)** Simulation results when the ice-ocean interface is at a depth of Top – 11 m (2.75 m x 2.75 m grid), Middle – 56 m (5.5 m x 5.5 m grid), and Bottom – 1084 m (27.5 m x 27.5 m grid). **(Left-Right)** Porosity (contours demarcate porosities of 0.15 to 0.95 in increments of 0.2), brine salinity, and absolute salinity gradient ($|\partial C/\partial x| + |\partial C/\partial y|$) profiles during the simulations. (Note: the scale of the color bars differs between some of the images so as to highlight gradients within individual images. Additionally, these images have been extracted from simulations spanning much larger domains, ensuring the mushy layer is not impacted by edge effects.)

physicochemical structure of the ice-ocean interface; and the potential implications the ice-ocean interface may have on habitability and geophysical processes.

Our work corroborates the work of Buffo et al. (2020) who implemented a one-dimensional reactive transport model to predict the bulk salinity profile of Europa's forming ice shell and the evolution of hydrological structures within the shell. The functional relationship between bulk salinity and depth within the ice shell derived by Buffo et al. (2020) captures the structure of the bulk salinity profile simulated in this study (Figure 3a-c). In the shallow shell substantial amounts of salt are retained in the forming ice, but as the ice shell thickens salt is more efficiently drained from the mushy layer and bulk salinity asymptotically approaches a nonzero lower limit. In congelation ice (ice formed due to conductive heat loss to the overlying ice shell), such as we simulate here, this lower limit is governed by the permeability of the mushy layer at low porosities. This is in contrast to marine ice (formed by the buoyant deposition and compaction of ice crystals formed in the water column (Lewis & Perkin, 1983; Buffo et al., 2021; Soderlund, 2019)), which more efficiently excludes solutes and has been observed to have salinities an order of magnitude lower (J. Tison et al., 2001). While an extremely important value in predicting the dynamics of the ice-ocean interface, permeability, and its relationship to porosity, is not well constrained (Buffo et al., 2020; Golden et al., 1998, 2007) and remains a contentious topic and active field of research (Freitag & Eicken, 2003; McCarthy et al., 2013; Petrich et al., 2006). Reduced permeability in the ice-ocean interfacial mushy layer or the existence of a percolation threshold below a critical ice porosity (e.g. (Golden et al., 2007, 1998)) would result in amplified impurity entrainment, while enhanced permeability would result in reduced impurity entrainment (see Supplementary Section S1 and Figure S3). Similarly, our results show that at high thermal gradients (>100 K/m) ice effectively traps all of the salt from the parent liquid (i.e. freezing is too rapid for salts to be expelled from the ice). Our results demonstrating the relationship between salt entrainment and interfacial thermal gradient (Figure 3d-f) are an improvement on the results of Buffo et al. (2020) whose one-dimensional model struggled with stability issues under thermal gradients >20 K/m.

We have shown that there exists a distinct and quantifiable relationship between the thermochemical environment of the ice-ocean interface at the time of solidification and the properties of the ice that forms. With the likelihood of ongoing hydrological activity within Europa's ice shell in the form of lenses (B. E. Schmidt et al., 2011; Spaun et al., 1998), sills (Chivers et al., 2020; Craft et al., 2016; Manga & Michaut, 2017; Michaut & Manga, 2014), dikes, fractures (Dombard et al., 2013; Rudolph & Manga, 2009; Walker et al., 2014), and plumes (Jia et al., 2018; Sparks et al., 2016) understanding the characteristics of ice formed in an array of thermal environments is imperative in constraining the mechanical, dielectric, and eutectic properties of refrozen features. The presence of salt alters the rheological properties of ice (Assur, 1958; Durham et al., 2005; McCarthy et al., 2011) and could facilitate the reactivation of fractures as well as the dynamics of solid-state convection in the ductile portion of the ice shell (e.g. Buffo et al. (2020)). Shallow lenses within the shell can be drastically affected by the dynamics of ice formation and salt entrainment/rejection. Separated from the underlying ocean, progressive freezeout of these features results in concentration of the residual brine, depressing the freezing point of the fluid, increasing the lens' longevity, and potentially resulting in the precipitation of salt hydrate layers when the reservoir reaches saturation (Buffo et al., 2020; Chivers et al., 2020). Ice penetrating radar observations depend critically on the dielectric properties of the ice shell (Di Paolo et al., 2016; Kalousová et al., 2017; Moore, 2000), thus detecting and distinguishing features within the ice shell as well as the ice-ocean interface relies on our understanding of the ice shell's composition.

Any chemical measurements of plume particles (e.g. Cassini's measurements of Enceladus' south polar plumes using the CDA (Hansen et al., 2011; Matson et al., 2007; Waite et al., 2017)) rely on assumptions about the origin of the particles (ocean derived or sourced from within the shell) and the quality of chemical signatures retained from the parent reservoir. Our results suggest that flash freezing at thermal gradients >100 K/m would produce ice particles that retain an exceptional chemical fingerprint of their parent fluid. However, if plume particles form through a more temperate process (e.g. slow ascension through a warm fracture (e.g. (J. Schmidt et al., 2008))) they may only preserve a fraction of the source fluid's composition. If the thermal environment in the region of particle generation is known, our results can be utilized to link particle chemistry observations to parent reservoir chemistry. Lastly, any ocean-surface transport will be mediated by impurity entrainment at the ice-ocean interface (Allu Peddinti & McNamara, 2015). Thus, constraining material entrainment rates is crucial to assessing the fluxes associated with potential chemical overturn within the ice shell that may facilitate disequilibrium chemistries favorable for life (Hand et al., 2007; Vance et al., 2016) and will govern observable biosignature delivery to the surface/upper ice shell (B. E. Schmidt, 2020).

Although there are important parallels between the ice-ocean interfaces of icy worlds and those found on Earth beneath sea ice and ice shelves (e.g. (Buffo et al., 2020; Greeley et al., 1998; Pappalardo & Coon, 1996)), there are important facets of their scale and structure which may facilitate unique processes not represented in terrestrial analog systems. For

Europa, the thickness of the ice shell (~10-30 km) coupled with a gravity approximately one tenth that of Earth (~1.32 m/s^2) leads to predicted ice-ocean interface mushy layer thicknesses of 537 m and 1611 m for a 10 km and 30 km thick ice shell, respectively (using equation 11 and the coefficients given in the caption of Figure 5). These thicknesses far exceed the ~10-30 cm thick mushy layers observed in sea ice (Feltham et al., 2006; Hunke et al., 2011; Worster & Rees Jones, 2015) and meters to tens of meters of hydraulic connectivity observed at the base of ice shelves (Craven et al., 2009; Zotikov et al., 1980). Moreover, if there exist other ocean impurities that further depress its eutectic temperature the ice-ocean interface mushy layer could be even thicker. It is important to note that these mushy layer thickness predictions are associated with an actively growing ice shell. It is possible that contemporary ice shells have reached a quasi-equilibrium thermal state (e.g. (Hussmann et al., 2002)) in which temporal and spatial patterns of thickening and thinning have conspired to produce a heterogeneous mushy layer (or lack thereof in regions which are thinning or have reached an equilibrium thickness) (Buffo et al., 2021). This has important implications for the geophysics and astrobiological potential of ice-ocean interface environments, a full account of which can be found in (Buffo et al., 2021).

With the likely global nature of Europa's ice-ocean interface, and its adjacency to the moon's ductile, likely convective, icy mantle (Barr & McKinnon, 2007; Han & Showman, 2005; McKinnon, 1999), we suggest that in a number of aspects it may be best thought of as a core-mantle phase boundary, akin to the D" layer of Earth. Existing as a multiphase layer, separating a denser fluid underlying a lighter solid (outer core and mantle, respectively), this elusive layer plays an integral role in Earth's geophysical evolution (Burke et al., 2008; Maruyama et al., 2007; Olson et al., 1987). In this analogy, regional topography and heterogeneous heat flow could drive ice dynamics mirroring diapiric mantle plumes and tectonic processes on Earth (Burke et al., 2008; Lay et al., 2008; Olson et al., 1987), both of which have been suggested by geomorphological observations of features on Europa's surface (Head et al., 1999; Kattenhorn & Hurford, 2009; Kattenhorn & Prockter, 2014; Pappalardo & Barr, 2004; Prockter et al., 2002; B. E. Schmidt et al., 2011). If this is the case, the multiphase ice-ocean boundary of Europa not only governs the rates of heat and mass transport between the two reservoirs via micro- and mesoscopic physics but may also dictate regional and global scale geophysical processes. With the importance the D" layer plays in magmatic and tectonic processes on Earth, and analogous cryovolcanism (ice shell hydrology) (Fagents et al., 2000; Sparks et al., 2017) and ice tectonism (Kattenhorn & Hurford, 2009; Kattenhorn & Prockter, 2014) likely occurring on Europa, constraining the structure and heterogeneity of the ice-ocean interface mushy layer promises to provide novel insight on the dynamics and evolution of icy worlds. Additionally, and perhaps surprisingly, the ice-ocean interface of Europa provides a more accessible (See NASA's SESAME project (Howell & Pappalardo, 2020)) analog of the terrestrial D" layer and could be used to explore hypotheses regarding the Earth's interior.

The porous and reactive nature of the ice-ocean interface would provide an exceptional niche for any biology in the oceans of icy satellites. As the location where surface derived oxidants would be introduced into the theoretically reduced ocean (Hand et al., 2007; Vance et al., 2016), the ice-ocean boundary layer of Europa would be rich in chemical gradients and disequilibria in an otherwise likely oligotrophic water column (less the ocean-rock interface ~100 km below) (Lipps & Rieboldt, 2005). This is in addition to the chemical gradients produced by ice formation (e.g. Section 3.3). On Earth, the basal surfaces of oceanic ices (sea ice, ice shelves) house a rich community of bacteria, algae and higher order heterotrophs (Daly et al., 2013; Gradinger et al., 1999; Loose et al., 2011; Spindler, 1994; Thomas & Dieckmann, 2003). On icy worlds, devoid of sunlight, any biotic systems will likely be fueled by chemolithoautotrophic primary producers (Hoover & Pikuta, 2010; Pikuta & Hoover, n.d.; B. E. Schmidt, 2020), similar to hydrothermal, deep benthic, and/or endolithic environments on Earth. In thick ice shells with permeable layers >1 km thick there may be an array of unique ice-ocean/brine sub-environments within these layers which could be colonized by extremophiles adapted to take advantage of regional sources of energy. With Europa's prominence amongst high priority astrobiology targets constraining the physicochemical dynamics and habitability of a long-lived (in comparison to shallow features) and accessible (in comparison to the seafloor) biologically favorable niche is in line with a multitude of NASA goals (NRC, 2012; Des Marais et al., 2008; Hendrix et al., 2019).

5 Conclusion

The ice-ocean interface of Europa and other icy worlds is likely characterized by a dynamic mushy zone consisting of porous ice and saline interstitial brine. Such reactive phase change boundaries play an integral role in both the biogeochemical cycling and geophysics of the Earth (Loose et al., 2011; Hunke et al., 2011). Similarly, as a likely ubiquitous feature on Europa and other icy satellites the ice-ocean interface dictates ocean-surface transport, the physicochemical characteristics of the ice shell, likely governs both regional and global geophysical processes, and may provide a gradient rich oasis for any resident organisms. Constraining the dynamics and properties of the ice-ocean interface will improve geophysical models of the ice shell, aid in the planning and synthesis of missions in the lens of planetary exploration and planetary protection directives, and help constrain the habitability of ice-ocean worlds.

Acknowledgments

Data Availability Statement: SOFTBALL and its associated documentation can be found in (J. R. G. Parkinson, Martin, & Buffo, 2020). All model input files used in this manuscript can be found in the repository directory 'mushy-layer/examples/europa' (J. R. G. Parkinson, Martin, & Buffo, 2020).

References

Ackley, S. F., & Sullivan, C. W. (1994). Physical controls on the development and characteristics of antarctic sea ice biological communities—a review and synthesis [Journal Article]. *Deep Sea Research Part I: Oceanographic Research Papers*, *41*(10), 1583-1604.

Allu Peddinti, D., & McNamara, A. K. (2015). Material transport across europa's ice shell [Journal Article]. *Geophysical Research Letters*, *42*(11), 4288-4293.

Assur, A. (1958). Composition of sea ice and its tensile strength [Journal Article]. *Arctic sea ice*, *598*, 106-138.

Barge, L. M., Abedian, Y., Doloboff, I. J., Nuñez, J. E., Russell, M. J., Kidd, R. D., & Kanik, I. (2015). Chemical gardens as flow-through reactors simulating natural hydrothermal systems [Journal Article]. *JoVE (Journal of Visualized Experiments)*(105), e53015.

Barr, A. C., & McKinnon, W. B. (2007). Convection in ice i shells and mantles with self-consistent grain size [Journal Article]. *Journal of Geophysical Research: Planets*, *112*(E2).

Bear, J. (2013). *Dynamics of fluids in porous media* [Book]. Courier Corporation.

Bierson, C. J., Nimmo, F., & Stern, S. A. (2020). Evidence for a hot start and early ocean formation on pluto [Journal Article]. *Nature Geoscience*. Retrieved from `https://doi.org/10.1038/s41561-020-0595-0` doi: 10.1038/s41561-020-0595-0

Brown, E. K., Buffo, J. J., Grantham, M., Pontefract, A., Glass, J., Ingall, E., . . . Carr, C. (2020). Trapped in the ice: An analysis of brines in british columbia's hypersaline lakes [Journal Article]. *LPI*(2326), 2218.

Buffo, J. J. (2019). *Multiphase reactive transport in planetary ices* (Thesis). Georgia Institute of Technology.

Buffo, J. J., Schmidt, B. E., Huber, C., & Meyer, C. R. (2021). Characterizing the ice-ocean interface of icy worlds: A theoretical approach. *Icarus*. doi: 10.1016/j.icarus.2021.114318

Buffo, J. J., Schmidt, B. E., Huber, C., & Walker, C. C. (2020). Entrainment and dynamics of ocean-derived impurities within europa's ice shell [Journal Article]. *JGR: Planets*.

Burke, K., Steinberger, B., Torsvik, T. H., & Smethurst, M. A. (2008). Plume generation zones at the margins of large low shear velocity provinces on the core–mantle boundary [Journal Article]. *Earth and Planetary Science Letters*, *265*(1-2), 49-60.

Cartwright, J. H. E., Escribano, B., González, D. L., Sainz-Díaz, C. I., & Tuval, I. (2013). Brinicles as a case of inverse chemical gardens [Journal Article]. *Langmuir*, *29*(25), 7655-7660.

Cartwright, J. H. E., García-Ruiz, J. M., Novella, M. L., & Otálora, F. (2002). Formation of chemical gardens [Journal Article]. *Journal of colloid and interface science*, *256*(2), 351-359.

Chivers, C. J., Buffo, J. J., & Schmidt, B. E. (2020). Thermal and chemical evolution of small, shallow water bodies on europa [Journal Article]. *LPI*(2326), 1047.

Chung, C., & Worster, M. G. (2002). Steady-state chimneys in a mushy layer [Journal Article]. *Journal of Fluid Mechanics*, *455*, 387.

Cottier, F., Eicken, H., & Wadhams, P. (1999). Linkages between salinity and brine channel distribution in young sea ice [Journal Article]. *Journal of Geophysical Research: Oceans*, *104*(C7), 15859-15871.

Cox, G. F. N., & Weeks, W. F. (1974). Salinity variations in sea ice [Journal Article]. *Journal of Glaciology*, *13*(67), 109-120.

Craft, K. L., Patterson, G. W., Lowell, R. P., & Germanovich, L. (2016). Fracturing and flow: Investigations on the formation of shallow water sills on europa [Journal Article]. *Icarus*, *274*, 297-313.

Craven, M., Allison, I., Fricker, H. A., & Warner, R. (2009). Properties of a marine ice layer under the amery ice shelf, east antarctica [Journal Article]. *Journal of Glaciology*, *55*(192), 717-728.

Daly, M., Rack, F., & Zook, R. (2013). Edwardsiella andrillae, a new species of sea anemone from antarctic ice [Journal Article]. *PloS one*, *8*(12), e83476.

Des Marais, D. J., Nuth, J. A., Allamandola, L. J., Boss, A. P., Farmer, J. D., Hoehler, T. M., ... Runnegar, B. (2008). The nasa astrobiology roadmap [Journal Article]. *Astrobiology*, *8*(4), 715-730.

Di Paolo, F., Lauro, S. E., Castelletti, D., Mitri, G., Bovolo, F., Cosciotti, B., ... Bruzzone, L. (2016). Radar signal penetration and horizons detection on europa through numerical simulations [Journal Article]. *IEEE Journal of Selected Topics in Applied Earth Observations and Remote Sensing*, *10*(1), 118-129.

Dombard, A. J., Patterson, G. W., Lederer, A. P., & Prockter, L. M. (2013). Flanking fractures and the formation of double ridges on europa [Journal Article]. *Icarus*, *223*(1), 74-81.

Durham, W. B., Stern, L. A., Kubo, T., & Kirby, S. H. (2005). Flow strength of highly hydrated mg-and na-sulfate hydrate salts, pure and in mixtures with water ice, with application to europa [Journal Article]. *Journal of Geophysical Research: Planets*, *110*(E12).

Eicken, H. (1992). Salinity profiles of antarctic sea ice: field data and model results [Journal Article]. *Journal of Geophysical Research: Oceans*, *97*(C10), 15545-15557.

Fagents, S. A., Greeley, R., Sullivan, R. J., Pappalardo, R. T., Prockter, L. M., & Team, G. S. (2000). Cryomagmatic mechanisms for the formation of rhadamanthys linea, triple band margins, and other low-albedo features on europa [Journal Article]. *Icarus*, *144*(1), 54-88.

Feltham, D. L., Untersteiner, N., Wettlaufer, J. S., & Worster, M. G. (2006). Sea ice is a mushy layer [Journal Article]. *Geophysical Research Letters*, *33*(14).

Fortes, A. D. (2000). Exobiological implications of a possible ammonia–water ocean inside titan [Journal Article]. *Icarus*, *146*(2), 444-452.

Freitag, J., & Eicken, H. (2003). Meltwater circulation and permeability of arctic summer sea ice derived from hydrological field experiments [Journal Article]. *Journal of Glaciology*, *49*(166), 349-358.

Golden, K. M., Ackley, S. F., & Lytle, V. (1998). The percolation phase transition in sea ice [Journal Article]. *Science*, *282*(5397), 2238-2241.
Golden, K. M., Eicken, H., Heaton, A. L., Miner, J., Pringle, D. J., & Zhu, J. (2007). Thermal evolution of permeability and microstructure in sea ice [Journal Article]. *Geophysical Research Letters*, *34*(16).
Gradinger, R., Friedrich, C., & Spindler, M. (1999). Abundance, biomass and composition of the sea ice biota of the greenland sea pack ice [Journal Article]. *Deep Sea Research Part II: Topical Studies in Oceanography*, *46*(6-7), 1457-1472.
Grasset, O., Dougherty, M. K., Coustenis, A., Bunce, E. J., Erd, C., Titov, D., ... Fletcher, L. N. (2013). Jupiter icy moons explorer (juice): An esa mission to orbit ganymede and to characterise the jupiter system [Journal Article]. *Planetary and Space Science*, *78*, 1-21.
Greeley, R., Sullivan, R., Coon, M. D., Geissler, P. E., Tufts, B. R., Head III, J. W., ... Moore, J. M. (1998). Terrestrial sea ice morphology: Considerations for europa [Journal Article]. *Icarus*, *135*(1), 25-40.
Hammond, N. P., Barr, A. C., & Parmentier, E. M. (2016). Recent tectonic activity on pluto driven by phase changes in the ice shell [Journal Article]. *Geophysical Research Letters*, *43*(13), 6775-6782.
Hammond, N. P., Parmenteir, E., & Barr, A. C. (2018). Compaction and melt transport in ammonia-rich ice shells: Implications for the evolution of triton [Journal Article]. *Journal of Geophysical Research: Planets*, *123*(12), 3105-3118.
Han, L., & Showman, A. P. (2005). Thermo-compositional convection in europa's icy shell with salinity [Journal Article]. *Geophysical research letters*, *32*(20).
Hand, K. P., Carlson, R. W., & Chyba, C. F. (2007). Energy, chemical disequilibrium, and geological constraints on europa [Journal Article]. *Astrobiology*, *7*(6), 1006-1022.
Hand, K. P., Chyba, C., Priscu, J., Carlson, R., & Nealson, K. (2009). Astrobiology and the potential for life on europa [Journal Article]. *Europa*, 589-629.
Hand, K. P., & Chyba, C. F. (2007). Empirical constraints on the salinity of the europan ocean and implications for a thin ice shell [Journal Article]. *Icarus*, *189*(2), 424-438.
Hansen, C., Shemansky, D. E., Esposito, L. W., Stewart, A., Lewis, B., Colwell, J., ... Teolis, B. (2011). The composition and structure of the enceladus plume [Journal Article]. *Geophysical Research Letters*, *38*(11).
Head, J. W., Pappalardo, R. T., & Sullivan, R. (1999). Europa: Morphological characteristics of ridges and triple bands from galileo data (e4 and e6) and assessment of a linear diapirism model [Journal Article]. *Journal of Geophysical Research: Planets*, *104*(E10), 24223-24236.
Hendrix, A. R., Hurford, T. A., Barge, L. M., Bland, M. T., Bowman, J. S., Brinckerhoff, W., ... Collins, G. C. (2019). The nasa roadmap to ocean worlds [Journal Article]. *Astrobiology*, *19*(1), 1-27.
Hoover, R. B., & Pikuta, E. V. (2010). Psychrophilic and psychrotolerant microbial extremophiles in polar environments [Journal Article].
Howell, S. M., & Pappalardo, R. T. (2018). Band formation and ocean-surface interaction on europa and ganymede [Journal Article]. *Geophysical Research Letters*, *45*(10), 4701-4709.
Howell, S. M., & Pappalardo, R. T. (2020). Nasa's europa clipper—a mission to a potentially habitable ocean world [Journal Article]. *Nature Communications*, *11*(1), 1-4.
Hunke, E., Notz, D., Turner, A., & Vancoppenolle, M. (2011). The multiphase physics of sea ice: a review for model developers [Journal Article]. *The Cryosphere*, *5*(4), 989-1009.
Hussmann, H., Spohn, T., & Wieczerkowski, K. (2002). Thermal equilibrium states of europa's ice shell: Implications for internal ocean thickness and surface heat flow [Journal Article]. *Icarus*, *156*(1), 143-151. Retrieved from `<GotoISI>://WOS:000175374300009` doi: 10.1006/icar.2001.6776
Jia, X., Kivelson, M. G., Khurana, K. K., & Kurth, W. S. (2018). Evidence of a plume on europa from galileo magnetic and plasma wave signatures [Journal Article]. *Nature Astronomy*, *2*(6), 459-464.

Johnson, B. C., Sheppard, R. Y., Pascuzzo, A. C., Fisher, E. A., & Wiggins, S. E. (2017). Porosity and salt content determine if subduction can occur in europa's ice shell [Journal Article]. *Journal of Geophysical Research: Planets*, *122*(12), 2765-2778.
Kalousová, K., Schroeder, D. M., & Soderlund, K. M. (2017). Radar attenuation in europa's ice shell: Obstacles and opportunities for constraining the shell thickness and its thermal structure [Journal Article]. *Journal of Geophysical Research: Planets*, *122*(3), 524-545.
Karani, H., & Huber, C. (2017). Transitional behaviour of convective patterns in free convection in porous media [Journal Article]. *Journal of Fluid Mechanics*, *818*.
Kargel, J. S., Kaye, J. Z., Head III, J. W., Marion, G. M., Sassen, R., Crowley, J. K., ... Hogenboom, D. L. (2000). Europa's crust and ocean: origin, composition, and the prospects for life [Journal Article]. *Icarus*, *148*(1), 226-265.
Kattenhorn, S. A., & Hurford, T. (2009). Tectonics of europa [Book Section]. In *Europa* (p. 199-236). University of Arizona Press Tucson.
Kattenhorn, S. A., & Prockter, L. M. (2014). Evidence for subduction in the ice shell of europa [Journal Article]. *Nature Geoscience*, *7*(10), 762.
Katz, R. F., & Worster, M. G. (2008). Simulation of directional solidification, thermochemical convection, and chimney formation in a hele-shaw cell [Journal Article]. *Journal of Computational Physics*, *227*(23), 9823-9840.
Khurana, K., Kivelson, M., Stevenson, D., Schubert, G., Russell, C., Walker, R., & Polanskey, C. (1998). Induced magnetic fields as evidence for subsurface oceans in europa and callisto [Journal Article]. *Nature*, *395*(6704), 777.
Kirk, R. L., Brown, R. H., & Soderblom, L. A. (1990). Subsurface energy storage and transport for solar-powered geysers on triton [Journal Article]. *Science*, *250*(4979), 424-429.
Lay, T., Hernlund, J., & Buffett, B. A. (2008). Core–mantle boundary heat flow [Journal Article]. *Nature geoscience*, *1*(1), 25.
Le Bars, M., & Worster, M. G. (2006). Interfacial conditions between a pure fluid and a porous medium: implications for binary alloy solidification [J. Fluid Mech.].
Lewis, E. L., & Perkin, R. G. (1983). Supercooling and energy exchange near the arctic ocean surface [Journal Article]. *Journal of Geophysical Research-Oceans*, *88*(Nc12), 7681-7685. Retrieved from `<GotoISI>://WOS:A1983RG83200017` doi: DOI10.1029/JC088iC12p07681
Lipps, J. H., & Rieboldt, S. (2005). Habitats and taphonomy of europa [Journal Article]. *Icarus*, *177*(2), 515-527.
Loose, B., Miller, L. A., Elliott, S., & Papakyriakou, T. (2011). Sea ice biogeochemistry and material transport across the frozen interface [Journal Article]. *Oceanography*, *24*(3), 202-218.
Mahadevan, K. (2017). *The growth and dynamics of brinicles* (Uundergraduate Thesis). School of Engineering and Applied Sciences, Harvard University.
Manga, M., & Michaut, C. (2017). Formation of lenticulae on europa by saucer-shaped sills [Journal Article]. *Icarus*, *286*, 261-269.
Marion, G. M., Fritsen, C. H., Eicken, H., & Payne, M. C. (2003). The search for life on europa: limiting environmental factors, potential habitats, and earth analogues [Journal Article]. *Astrobiology*, *3*(4), 785-811.
Maruyama, S., Santosh, M., & Zhao, D. (2007). Superplume, supercontinent, and post-perovskite: mantle dynamics and anti-plate tectonics on the core–mantle boundary [Journal Article]. *Gondwana Research*, *11*(1-2), 7-37.
Matson, D. L., Castillo, J. C., Lunine, J., & Johnson, T. V. (2007). Enceladus' plume: Compositional evidence for a hot interior [Journal Article]. *Icarus*, *187*(2), 569-573.
McCarthy, C., Blackford, J., & Jeffree, C. (2013). Low-temperature-sem study of dihedral angles in the ice-i/sulfuric acid partially molten system [Journal Article]. *Journal of microscopy*, *249*(2), 150-157.
McCarthy, C., Cooper, R. F., Goldsby, D. L., Durham, W. B., & Kirby, S. H. (2011). Transient and steady state creep response of ice i and magnesium sulfate hydrate eutectic

aggregates [Journal Article]. *Journal of Geophysical Research: Planets*, *116*(E4).
McCarthy, C., Cooper, R. F., Kirby, S. H., Rieck, K. D., & Stern, L. A. (2007). Solidification and microstructures of binary ice-i/hydrate eutectic aggregates [Journal Article]. *American Mineralogist*, *92*(10), 1550-1560.
McKinnon, W. B. (1999). Convective instability in europa's floating ice shell [Journal Article]. *Geophysical Research Letters*, *26*(7), 951-954.
McKinnon, W. B., & Kirk, R. L. (2014). Triton [Book Section]. In *Encyclopedia of the solar system* (p. 861-881). Elsevier.
Michaut, C., & Manga, M. (2014). Domes, pits, and small chaos on europa produced by water sills [Journal Article]. *Journal of Geophysical Research: Planets*, *119*(3), 550-573.
Middleton, C., Thomas, C., Escala, D., Tison, J.-L., & De Wit, A. (2015). Imaging the evolution of brine transport in experimentally grown quasi-two-dimensional sea ice [Journal Article]. *Procedia IUTAM*, *15*, 95-100.
Moore, J. C. (2000). Models of radar absorption in europan ice [Journal Article]. *Icarus*, *147*(1), 292-300.
Nakawo, M., & Sinha, N. K. (1981). Growth rate and salinity profile of first-year sea ice in the high arctic [Journal Article]. *Journal of Glaciology*, *27*(96), 315-330.
Nimmo, F. (2020). Solving the puzzle of enceladus's active south pole [Journal Article]. *Proceedings of the National Academy of Sciences*, *117*(28), 16107-16108.
Nimmo, F., & Pappalardo, R. (2016). Ocean worlds in the outer solar system [Journal Article]. *Journal of Geophysical Research: Planets*, *121*(8), 1378-1399.
Notz, D., Wettlaufer, J. S., & Worster, M. G. (2005). A non-destructive method for measuring the salinity and solid fraction of growing sea ice in situ [Journal Article]. *Journal of Glaciology*, *51*(172), 159-166.
NRC. (2012). *Vision and voyages for planetary science in the decade 2013-2022* [Book]. National Academies Press.
Olson, P., Schubert, G., & Anderson, C. (1987). Plume formation in the d "-layer and the roughness of the core–mantle boundary [Journal Article]. *Nature*, *327*(6121), 409.
Pappalardo, R. T., & Barr, A. C. (2004). The origin of domes on europa: The role of thermally induced compositional diapirism [Journal Article]. *Geophysical Research Letters*, *31*(1).
Pappalardo, R. T., & Coon, M. (1996). A sea ice analog for the surface of europa [Conference Proceedings]. In *Lunar and planetary science conference* (Vol. 27).
Pappalardo, R. T., Senske, D., Korth, H., Klima, R., Vance, S., & Craft, K. (2017). The europa clipper mission: Exploring the habilatbility of a unique icy world [Conference Proceedings]. In *European planetary science congress* (Vol. 11).
Parkinson, C. D., Liang, M.-C., Yung, Y. L., & Kirschivnk, J. L. (2008). Habitability of enceladus: planetary conditions for life [Journal Article]. *Origins of Life and Evolution of Biospheres*, *38*(4), 355-369.
Parkinson, J. R. G. (2019). *Nonlinear convection in sea ice and other mushy layers* (Thesis). University of Oxford.
Parkinson, J. R. G., Martin, D., & Buffo, J. (2020, October). *jrgparkinson/mushy-layer: Code and input files for Europa simulations.* Zenodo. Retrieved from `https://doi.org/10.5281/zenodo.4118549` doi: 10.5281/zenodo.4118549
Parkinson, J. R. G., Martin, D. F., Wells, A. J., & Katz, R. F. (2020). Modelling binary alloy solidification with adaptive mesh refinement [Journal Article]. *Journal of Computational Physics: X*, *5*, 100043.
Petrich, C., Langhorne, P. J., & Sun, Z. F. (2006). Modelling the interrelationships between permeability, effective porosity and total porosity in sea ice [Journal Article]. *Cold Regions Science and Technology*, *44*(2), 131-144.
Pikuta, E. V., & Hoover, R. B. (n.d.). Astrobiological significance of chemolithoautotrophic acidophiles [Conference Proceedings]. In *Instruments, methods, and missions for astrobiology vii* (Vol. 5163, p. 179-190). International Society for Optics and Photonics.
Porco, C., Helfenstein, P., Thomas, P., Ingersoll, A., Wisdom, J., West, R., ... Roatsch, T.

(2006). Cassini observes the active south pole of enceladus [Journal Article]. *science*, *311*(5766), 1393-1401.

Prockter, L. M., Head, J. W., Pappalardo, R. T., Sullivan, R. J., Clifton, A. E., Giese, B., ... Neukum, G. (2002). Morphology of europan bands at high resolution: A mid-ocean ridge-type rift mechanism [Journal Article]. *Journal of Geophysical Research: Planets*, *107*(E5).

Rees Jones, D. W., & Worster, M. G. (2013). A simple dynamical model for gravity drainage of brine from growing sea ice [Journal Article]. *Geophysical Research Letters*, *40*(2), 307-311.

Rudolph, M. L., & Manga, M. (2009). Fracture penetration in planetary ice shells [Journal Article]. *Icarus*, *199*(2), 536-541.

Santibáñez, P. A., Michaud, A. B., Vick-Majors, T. J., D'Andrilli, J., Chiuchiolo, A., Hand, K. P., & Priscu, J. C. (2019). Differential incorporation of bacteria, organic matter, and inorganic ions into lake ice during ice formation [Journal Article]. *Journal of Geophysical Research: Biogeosciences*.

Schmidt, B. E. (2020). The astrobiology of europa and the jovian system [Journal Article]. *Planetary Astrobiology*, 185.

Schmidt, B. E., Blankenship, D., Patterson, G., & Schenk, P. (2011). Active formation of 'chaos terrain'over shallow subsurface water on europa [Journal Article]. *Nature*, *479*(7374), 502.

Schmidt, B. E., Buffo, J., & Main Campus, A. (n.d.). Biomarker production and preservation on europa [Conference Proceedings]. In *European planetary science congress* (Vol. 11).

Schmidt, J., Brilliantov, N., Spahn, F., & Kempf, S. (2008). Slow dust in enceladus' plume from condensation and wall collisions in tiger stripe fractures [Journal Article]. *Nature*, *451*(7179), 685-688.

Schroeder, D. M., Romero-Wolf, A., Carrer, L., Grima, C., Campbell, B. A., Kofman, W., ... Blankenship, D. D. (2016). Assessing the potential for passive radio sounding of europa and ganymede with rime and reason [Journal Article]. *Planetary and Space Science*, *134*, 52-60.

Schubert, G., Anderson, J., Spohn, T., & McKinnon, W. (2004). Interior composition, structure and dynamics of the galilean satellites [Journal Article]. *Jupiter: The planet, satellites and magnetosphere*, *1*, 281-306.

Soderlund, K. M. (2019). Ocean dynamics of outer solar system satellites [Journal Article]. *Geophysical Research Letters*, *46*(15), 8700-8710. Retrieved from `<GotoISI>://WOS:000483812500013` doi: 10.1029/2018gl081880

Soderlund, K. M., Schmidt, B. E., Wicht, J., & Blankenship, D. D. (2014). Ocean-driven heating of europa's icy shell at low latitudes [Journal Article]. *Nature Geoscience*, *7*(1), 16-19. Retrieved from `<GotoISI>://WOS:000328962700012` doi: 10.1038/Ngeo2021

Sotin, C., Head III, J. W., & Tobie, G. (2002). Europa: Tidal heating of upwelling thermal plumes and the origin of lenticulae and chaos melting [Journal Article]. *Geophysical Research Letters*, *29*(8), 74-1-74-4.

Sparks, W. B., Hand, K., McGrath, M., Bergeron, E., Cracraft, M., & Deustua, S. (2016). Probing for evidence of plumes on europa with hst/stis [Journal Article]. *The Astrophysical Journal*, *829*(2), 121.

Sparks, W. B., Schmidt, B. E., McGrath, M. A., Hand, K. P., Spencer, J. R., Cracraft, M., & Deustua, S. E. (2017). Active cryovolcanism on europa? [Journal Article]. *The Astrophysical Journal Letters*, *839*(2), L18.

Spaun, N., Head, J., Collins, G., Prockter, L., & Pappalardo, R. (1998). Conamara chaos region, europa: Reconstruction of mobile polygonal ice blocks [Journal Article]. *Geophysical research letters*, *25*(23), 4277-4280.

Spindler, M. (1994). Notes on the biology of sea ice in the arctic and antarctic [Journal Article]. *Polar Biology*, *14*(5), 319-324.

Steefel, C. I., DePaolo, D. J., & Lichtner, P. C. (2005). Reactive transport modeling: An essential tool and a new research approach for the earth sciences [Journal Article]. *Earth and Planetary Science Letters*, *240*(3-4), 539-558.

Tedesco, L., & Vichi, M. (2014). Sea ice biogeochemistry: A guide for modellers [Journal Article]. *PloS one*, *9*(2), e89217.

Thomas, D. N., & Dieckmann, G. S. (2003). Biogeochemistry of antarctic sea ice [Book Section]. In *Oceanography and marine biology, an annual review, volume 40* (p. 151-156). CRC Press.

Thomas, D. N., & Dieckmann, G. S. (2008). *Sea ice: an introduction to its physics, chemistry, biology and geology* [Book]. John Wiley & Sons.

Tison, J., Khazendar, A., & Roulin, E. (2001). A two-phase approach to the simulation of the combined isotope/salinity signal of marine ice [Journal Article]. *Journal of Geophysical Research: Oceans*, *106*(C12), 31387-31401.

Tison, J.-L., & Verbeke, V. (2001). Chlorinity/salinity distribution patterns in experimental granular sea ice [Journal Article]. *Annals of Glaciology*, *33*, 13-20.

Trumbo, S. K., Brown, M. E., & Hand, K. P. (2019). Sodium chloride on the surface of europa [Journal Article]. *Science advances*, *5*(6), eaaw7123.

Vance, S. D., Barge, L. M., Cardoso, S. S., & Cartwright, J. H. (2019). Self-assembling ice membranes on europa: Brinicle properties, field examples, and possible energetic systems in icy ocean worlds [Journal Article]. *arXiv preprint arXiv:1903.01584*.

Vance, S. D., & Brown, J. M. (2013). Thermodynamic properties of aqueous mgso$_4$ to 800 mpa at temperatures from -20 to 100° c and concentrations to 2.5 mol kg^{-1} from sound speeds, with applications to icy world oceans [Journal Article]. *Geochimica et Cosmochimica Acta*, *110*, 176-189.

Vance, S. D., Hand, K. P., & Pappalardo, R. T. (2016). Geophysical controls of chemical disequilibria in europa [Journal Article]. *Geophysical Research Letters*, *43*(10), 4871-4879.

Vance, S. D., Journaux, B., Hesse, M., & Steinbrügge, G. (2020). The salty secrets of icy ocean worlds [Journal Article]. *Journal of Geophysical Research: Planets*, e2020JE006736.

Waite, J. H., Glein, C. R., Perryman, R. S., Teolis, B. D., Magee, B. A., Miller, G., ... Bouquet, A. (2017). Cassini finds molecular hydrogen in the enceladus plume: evidence for hydrothermal processes [Journal Article]. *Science*, *356*(6334), 155-159.

Wakatsuchi, M., & Saito, T. (1985). On brine drainage channels of young sea ice [Journal Article]. *Annals of glaciology*, *6*, 200-202.

Walker, C., Schmidt, B., & Bassis, J. (2014). Breaking the ice: On the application of fracture system mechanics and fragmentation theory to the chaos regions of europa [Journal Article]. *LPI*(1777), 2659.

Wells, A. J., Hitchen, J. R., & Parkinson, J. R. (2019). Mushy-layer growth and convection, with application to sea ice [Journal Article]. *Philosophical Transactions of the Royal Society A*, *377*(2146), 20180165.

Wells, A. J., Wettlaufer, J., & Orszag, S. (2011). Brine fluxes from growing sea ice [Journal Article]. *Geophysical Research Letters*, *38*(4).

Wells, A. J., Wettlaufer, J. S., & Orszag, S. A. (2012). Nonlinear mushy-layer convection with chimneys: stability and optimal solute fluxes [Journal Article]. *arXiv preprint arXiv:1205.0964*.

Wettlaufer, J., Worster, M. G., & Huppert, H. E. (1997). Natural convection during solidification of an alloy from above with application to the evolution of sea ice [Journal Article]. *Journal of fluid mechanics*, *344*, 291-316.

Worster, M. G. (1991). Natural convection in a mushy layer [Journal Article]. *Journal of fluid mechanics*, *224*, 335-359.

Worster, M. G. (1997). Convection in mushy layers [Journal Article]. *Annual Review of Fluid Mechanics*, *29*(1), 91-122.

Worster, M. G., & Rees Jones, D. W. (2015). Sea-ice thermodynamics and brine drainage [Journal Article]. *Philosophical Transactions of the Royal Society A: Mathematical, Physical and Engineering Sciences*, *373*(2045), 20140166.

Zolotov, M. Y., & Kargel, J. (2009). *On the chemical composition of europa's icy shell, ocean, and underlying rocks* (Vol. 431) [Book]. University of Arizona Press Tucson,

AZ.
Zolotov, M. Y., & Shock, E. L. (2001). Composition and stability of salts on the surface of europa and their oceanic origin [Journal Article]. *Journal of Geophysical Research: Planets*, *106*(E12), 32815-32827.
Zotikov, I. A., Zagorodnov, V. S., & Raikovsky, J. V. (1980). Core drilling through the ross ice shelf (antarctica) confirmed basal freezing [Journal Article]. *Science*, *207*(4438), 1463-1465.